Dendronized Rigid−Flexible Macromolecular Architectures: Syntheses, Structure, and Properties in Bulk

A. K. Andreopoulou,[†] B. Carbonnier,[‡] J. K. Kallitsis,*[,†] and T. Pakula*[,‡]

Department of Chemistry, University of Patras, GR-265 00 Patras, Greece, and Foundation for Research and Technology-Hellas, Institute of Chemical Engineering and High-Temperature Chemical Processes, P. O. Box 1414, GR-265 00 Patras, Greece, and Max-Planck-Institute for Polymer Research, Postfach 3148, 55021 Mainz, Germany

Received November 10, 2003; Revised Manuscript Received March 1, 2004

ABSTRACT: Side-chain dendronized polymers consisting of regularly segmented alternating rigid−flexible main-chain units and side dendritic wedges are synthesized and analyzed in their bulk state using various experimental methods. High molecular weight polymers were obtained in most cases enabling the formation of self-supporting films. The thermal and mechanical characterization of these polymers, by means of DSC and dynamic mechanical analyses, has revealed a highly ordered nature, which was further supported from SALS and POM experiments. Additionally, their transition temperatures seem to strongly depend on the main-chain flexible spacer's length, in a manner resembling the odd−even effect. The existence of organizational features in both isotropic and macroscopically oriented samples was concluded for these polymeric materials due to the intense and well-resolved diffractions in their WAXS patterns. From qualitative analyses of the WAXS patterns corresponding to oriented filaments, the development of layered structures is postulated, comprised of main-chain polymeric backbones while the side dendrons occupy the space between the layers. Actually, two types of LC ordering for the extended backbones within the main-chain layers could be distinguished. In general, the exact polymeric structure, side-dendrons' generation and main-chain flexible spacers' length, greatly influence the final polymeric properties, such as phase transitions and structural parameters.

Introduction

The development of well-defined molecular and supramolecular architectures still attracts increasing scientific interest. Numerous pathways have so far been adopted trying to mimic nature's wiseness toward complicated, self-assembled, and self-organized materials.[1] Dendrimers, dendrons, and side-chain dendritic polymers offer unique opportunities for the development of such novel and complex macromolecular entities due to their evolutionary spherical or cylindrical shapes, great number of building blocks, and the possibility of several different functionalities coexisting in close proximity.[2,3] The delicate organization of many such macromolecules in larger self-assembled, self-organized systems is an intriguing aspect in dendrimer chemistry and physics. The specific molecular architecture and intermolecular interactions can control the microphase separation, aggregation phenomena, and order−disorder situations that are essential for the arrangement of these giant macromolecular species to a supramolecular structure.[4−7]

Inserting different, incompatible moieties into a macromolecular chain while at the same time allowing mobility into the system for ordered conformations finally to be adopted is a well-known "trick" for fabricating macroscopically organized materials.[8] In particular, rigid−flexible combinations may give rise to separation tendencies into a system due to the incompatibility of the segmental units. Such rod−coil molecules have so far been well investigated although precise macromolecular rigid−flexible alternating systems are still rare. Moreover, the introduction of side-chain moieties that show good compatibility with one or the other main-chain subunit could lead to even more complex architectures where the molecules tend to organize on the basis of the miscibility of the different segments.[8]

This work focuses on a novel combination of the above perspectives, in which side-chain dendritic polymers consisting of rigid−flexible main-chain units and side dendritic wedges were investigated. These dendronized polyethers, prepared by the convergent "macromonomer" approach,[3,9] bear terphenyl main-chain units, carrying two side dendrons in their middle phenylene ring, connected through aliphatic spacers of various lengths. Thus, these polymeric series offer the possibility of creating LC phases, since they contain the mesogenic terphenyl units distributed along the main polymeric backbones in a regular motive through the interfering aliphatic segments. It is these aliphatic segments that should provide flexibility into the system allowing for favorable conformations to be adopted by the macromolecular chains depending on space requirements imposed from the accommodation of such large side dendritic substituents. Moreover, the selected dendrons bear lengthy alkoxy chains at their periphery, resembling those of the Percec type,[5,6,10,11] in an effort to increase segregation and organization phenomena occurring due to the terphenyl and the aliphatic segments of the main chain and due to the alkoxy periphery groups and the phenylene branching points within the dendrons themselves. Actually, a variety of alkoxy periphery functionalized dendrons and dendrimers[11] as well as dendronized polymers[12−15] have been reported in the literature. Investigation of such polymeric systems has been performed mostly concerning their conformational behavior,[16] polymerization kinetics,[5,12] and optical properties.[14−17] Most interestingly, a pattern seems to dominate the polymers' organization: a pro-

[†] University of Patras.
[‡] Max-Planck-Institute for Polymer Research.
* Corresponding authors.

10.1021/ma035688p CCC: $27.50
Published on Web 04/10/2004

Scheme 1. (i) K_2CO_3, Acetone, Reflux for 12 h, 80% (G_1), or 24 h, 70% (G_2); (ii) for 2(G_1) $Pd(PPh)_3$, Toluene, Na_2CO_3 2 M, reflux for 24 h, 90%; (iii) for 2(G_2) $PdCl_2$(dppf), THF, NaOH 3 M, Reflux for 48 h, 70%; (iv) CSA, THF, MeOH, 18 h, 75% (G_1), 60% (G_2)

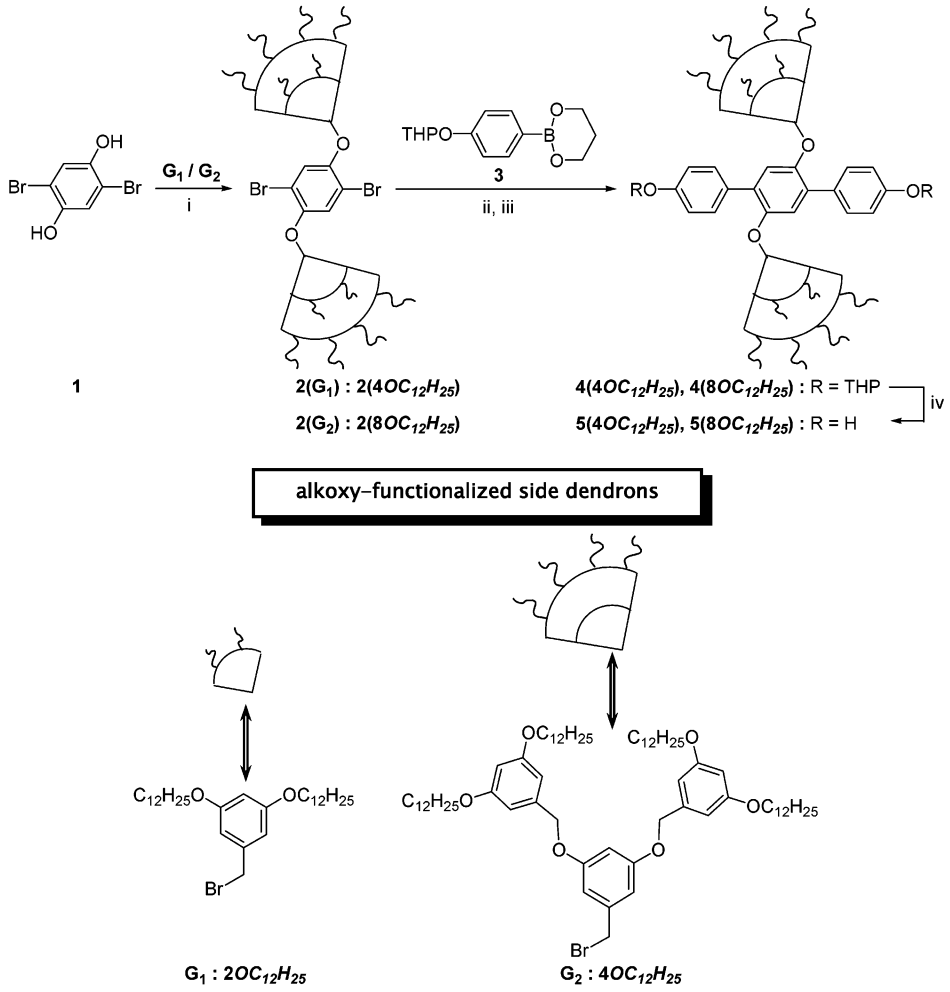

Scheme 2 (i) *o*-DCB, NaOH 10 N, TBAH, 120 °C, 2−4 days (G_1), 4−8 days (G_2)

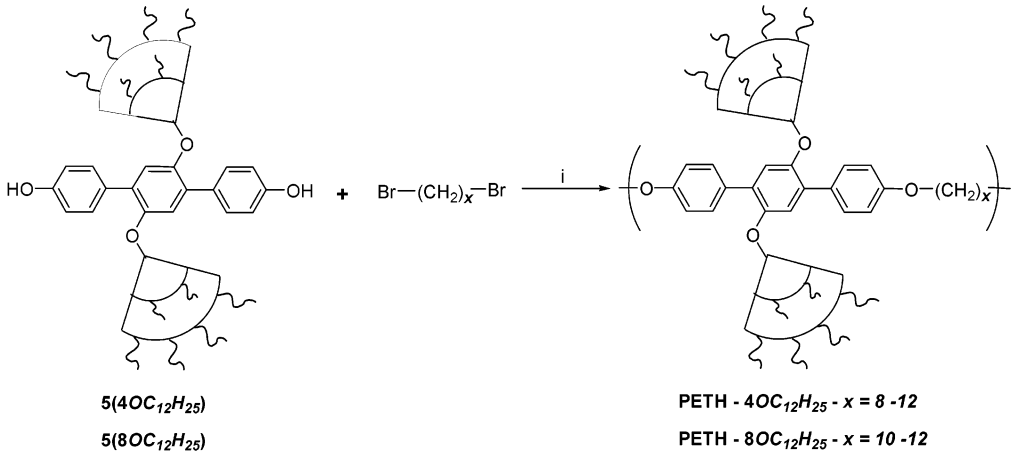

nounced tendency toward ordered structures with the dendrons self-packing, thus forcing the polymeric backbones to adopt specific arrangements.

In an effort to evaluate and understand our dendronized polymers and at the same time to discriminate differentiations from other already reported ones, various experimental techniques have been combined aiming especially at their bulk properties' characterization. Consequently, the effect of the main-chain flexible spacers' length and of the dendrons' generation on properties and structures developed has been thoroughly investigated.

Experimental Section

Materials. Dendrons $\mathbf{G_1}$ and $\mathbf{G_2}$,[10] 1,4-dihydroxy-2,5-dibromobenzene (**1**),[18] and catalysts $Pd(PPh_3)_4$[19] and $PdCl_2$(dppf)[20] were prepared according to literature procedures. The synthesis of 2-tetrahydropyranyloxy-4-phenylboronic acid (**3**) was described in a previous publication.[21] Tetrahydrofuran (THF) was distilled from sodium prior to use. Solvents of analytical

Table 1. Molecular Characteristics for the Synthesized Polyethers[a]

x	M_n[b]	M_w[b]	M_w/M_n[b]	Mru	DP[c]
		PETH-4OC$_{12}$H$_{25}$-*x*			
12[d]	45 700	103 140	2.3	1376	33.2
11[d]	61 400	151 290	2.5	1362	45.1
10[e]	50 300	146 830	2.9	1348	37.3
9[d]	60 200	126 360	2.1	1334	45.1
8[f]	27 490	85 450	3.1	1320	20.8
		PETH-8OC$_{12}$H$_{25}$-*x*			
12[g]	32 240	90 850	2.8	2536	12.7
11[h]	16 950	40 250	2.4	2522	6.7
10[e]	11 970	25 650	2.2	2508	4.8

[a] See Experimental Section for detailed synthetic procedures. [b] From GPC with a UV detector, $CHCl_3$ as eluent, and PS standards. [c] Number-average degree of polymerization calculated by dividing M_n values with the theoretical molecular weights of the monomer units (Mru) of the corresponding polyether. [d] Polymerization at 120 °C, 3 days. [e] Polymerization at 120 °C, 4 days. [f] Polymerization at 120 °C, 2 days. [g] Polymerization at 120 °C, 8 days. [h] Polymerization at 120 °C, 5 days.

grade purity were purchased from Aldrich or Merck and were used without further purification unless otherwise noted. The reagents 18-crown-6 (for synthesis), tetrabutylammonium hydrogen sulfate (TBAH) (97+%, T), (1*R*)-(−)-10-camphorosulfonic acid (CSA) (98%), K_2CO_3−NaOH−Na_2CO_3 (pro analyses), and aliphatic dibromides [$x = 11$ (98+%), $x = 9$ (97%), $x = 8$ (98%)] were supplied from Aldrich and used as received. Aliphatic dibromides $x = 12$ and $x = 10$ were recrystallized from methanol. All reactions were performed under an argon atmosphere. Degassing of reaction mixtures was performed by subsequent evacuations and filling with argon, cycles for three times.

Instrumentation. ^{1}H and ^{13}C NMR spectra were obtained on a Bruker Avance DPX spectrometer at 400 and 100 MHz, respectively, with deuterated $CHCl_3$ and DMSO with TMS as internal standard. Gel permeation chromatography (GPC) measurements were carried out using a Polymer Lab chromatographer with two Ultra Styragel linear columns with pore sizes of 10^4 and 500 Å, UV detector (254 nm), polystyrene standards, and $CHCl_3$ as eluent, at 25 °C with a flow rate of 1 mL/min.

Wide-angle X-ray diffraction (WAXS) patterns were recorded using the X-ray beam with a pinhole collimation and a two-dimensional detector (Siemens) with 1024 × 1024 pixels. A double graphite monochromator for the Cu Kα radiation (λ = 0.154 nm) was used. The beam diameter was about 0.5 mm, and the sample-to-detector distance was 80 mm. The recorded scattered intensity distributions were integrated over the azimuthal angle and are presented as functions of the scattering vector ($s = 2 \sin \theta/\lambda$, where 2θ is the scattering angle).

Differential scanning calorimetry (DSC) experiments were conducted with cooling and heating rates of 10 K/min using a Mettler 30 calorimeter with a cell purged with nitrogen. Calibration for the temperature and enthalpy changes was performed using indium as a standard. The second heating run is considered as reflecting the properties of the compact bulk material. Melting and crystallization temperatures (T_m and T_c, respectively) were determined at the peak maxima or from the tangent at the T_m peak, as explained in Table 2.

Dynamic mechanical measurements have been performed using a Rheometrics RMS 800 mechanical spectrometer. Shear deformation was applied under conditions of controlled deformation amplitude which was changed with temperature between $\Delta\gamma = 0.0001$ at low temperatures and $\Delta\gamma = 0.05$ at high temperatures, always remaining in the range of the linear viscoelastic response of studied samples. Plate−plate geometry has been used with plate diameters of 6 mm. The gap between plates (sample thickness) was about 1 mm. Experiments have been performed under a dry nitrogen atmosphere. Results are presented as temperature dependencies of the storage (G') and loss (G'') shear modulus measured at a constant deformation frequency of 10 rad/s. The results below 50 °C were obtained with a 2 °C/min cooling rate and above 50 °C with a 2 °C/min heating rate.

Table 2. Thermal Analyses of Polyethers PETH-4OC$_{12}$H$_{25}$-*x*[a]

Second Heating

x	T_m	T_c
12	84.8 (91) {7.2/28.7}	49.7 {20.8}
11	98 (103.0) {42.9}	56.2 {44.4}
10	95 (100.1) {30.6}	57 {36.2}
9	98.2 (102.5) {38.1}	65.8 {40.3}
8	104.3 (109.3) {47.5}	73.5 {47.6}

First Heating[b]

x	T_{m_a}	T_m	T_c
12	45.7	78.2	43
11	51	87.5/94.8	52
10	49.9	93.9 {28.6}	53.7
9	50.4	97.3 {26.0}	60.7
8	49.9	104 {30.1}	68.3

[a] T_{m_a}, T_m, T_c = at the peak maximum. T_m and T_{m_a} from the heating run. T_c from the cooling run. (T) = from the tangent at the T_m peak. {ΔH} = kJ/mru. [b] After aging of the samples for 3 months at room temperature.

Polarized optical microscopy (POM) observations were performed using a Zeiss microscope (D-7082) equipped with a temperature-controlled stage (Linkam TMS91/THM600) and a color digital camera (Hitachi KPD50). Small-angle light scattering (SALS) experiments were conducted with a He−Ne laser (λ = 633 nm) beam and a CCD camera (Hamamatsu) recording the 2D scattering patterns under Hv polarization conditions. To determine spherulite sizes, the scattered intensity distributions vs scattering angle were analyzed.[22]

1,4-Di[3,5-bis(dodecyloxy)benzyloxy]-2,5-dibromobenzene (2(4OC$_{12}$H$_{25}$)). A mixture of **1** (1.00 g, 3.73 mmol), dendron **G$_1$** (4.42 g, 8.20 mmol), K_2CO_3 (1.29 g, 9.35 mmol), and 18-crown-6 (0.20 g, 0.76 mmol) in acetone (100 mL) was refluxed for 18 h. The solvent was evaporated under reduced pressure and the mixture dispersed in H_2O (150 mL) and stirred for 12 h. Filtration, washing with H_2O, drying under vacuum, and recrystallization from *n*-hexane afforded **2(4OC$_{12}$H$_{25}$)** as a white powder. Yield 3.56 g (80%). Anal. Calcd for $C_{68}H_{112}O_6Br_2$ (1184): C, 68.92; H, 9.46. Found: C, 68.94; H, 9.68. ^{1}H NMR ($CDCl_3$): 0.88 (t, 12H, C*H*$_3$), 1.26−1.38 (m, 64H, CH$_3$(C*H*$_2$)$_8$), 1.42 (m, 8H, CH$_3$(CH$_2$)$_8$C*H*$_2$), 1.77 (m, 8H, CH$_3$(CH$_2$)$_8$CH$_2$C*H*$_2$), 3.94 (t, 8H, CH$_2$C*H*$_2$O), 5 (s, 4H, ArC*H*$_2$O), 6.4 (t, 2H, dendritic Ar−*H*), 6.58 (d, 4H, dendritic Ar−*H*), 7.15 (s, 2H, Ar−*H*). ^{13}C NMR ($CDCl_3$): 14.46 (*C*H$_3$), 23.04 (CH$_3$*C*H$_2$), 26.42 (CH$_3$CH$_2$*C*H$_2$), 29.61−29.99 (CH$_3$CH$_2$CH$_2$(*C*H$_2$)$_7$), 32.28 (CH$_3$CH$_2$CH$_2$(CH$_2$)$_7$*C*H$_2$), 68.52 (CH$_2$*C*H$_2$O), 72.35 (Ar*C*H$_2$O), 101.50 (OC*C*HCO), 105.77 (OC*C*HCCH$_2$O), 111.94 (Br*C*), 119.66 (BrC*C*H), 138.70 (CH*C*CH$_2$O), 150.45 (O*C*CBr), 160.92 (CH$_2$CH$_2$O*C*CH).

1,4-Di[3,5-bis(3,5-bis(dodecyloxy)benzyloxy)benzyloxy]-2,5-dibromobenzene (2(8OC$_{12}$H$_{25}$)). A mixture of **1** (0.50 g, 1.86 mmol), dendron G$_2$ (4.37 g, 3.91 mmol), K_2CO_3 (0.64 g, 4.60 mmol), and 18-crown-6 (98.60 mg, 0.37 mmol) in acetone (80 mL) was refluxed for 24 h. Filtration and evaporation of the solvent under reduced pressure afforded **2(8OC$_{12}$H$_{25}$)** as a viscous oil that crystallized upon standing and was used without further purification. Yield 3.06 g (70%). ^{1}H NMR ($CDCl_3$): 0.87 (t, 24H, C*H*$_3$), 1.26−1.38 (m, 128H, CH$_3$(C*H*$_2$)$_8$), 1.41 (m, 16H, CH$_3$(CH$_2$)$_8$C*H*$_2$), 1.76 (m, 16H, CH$_3$(CH$_2$)$_8$-CH$_2$C*H*$_2$), 3.93 (t, 16H, CH$_2$C*H*$_2$O), 4.95 (s, 8H, ArC*H*$_2$O), 5 (s, 4H, ArC*H*$_2$O), 6.39 (t, 4H, dendritic Ar−*H*), 6.56 (m, 10H,

dendritic Ar−*H*), 6.7 (d, 4H, dendritic Ar−*H*), 7.15 (s, 2H, Ar−*H*). ^{13}C NMR ($CDCl_3$): 14.54 (CH_3), 23.11 (CH_3CH_2), 26.47 ($CH_3CH_2CH_2$), 29.68−30.09 ($CH_3CH_2CH_2(CH_2)_7$), 32.33 ($CH_3CH_2CH_2(CH_2)_7CH_2$), 68.48 (CH_2CH_2O), 70.59 ($ArCH_2O$), 72.09 ($ArCH_2O$), 101.21 (OC*C*HCO), 102.19 (OC*C*HCO), 106.11 (OC*C*HCCH$_2$O), 106.29 (OC*C*HCCH$_2$O), 111.88 (Br*C*), 119.42 (Br*C*CH), 138.91 (OCH$_2$*C*CH), 139.30 (OCH$_2$*C*CH), 150.34 (O*C*CBr), 160.55 (CH*C*OCH$_2$Ar), 160.92 (CH$_2$CH$_2$O*C*CH).

2′,5′-Di[3,5-bis(dodecyloxy)benzyloxy]-*p*-triphenylene-4′,4″-di(tetrahydropyranyloxy) (4(4OC$_{12}$H$_{25}$)). A mixture containing **2(4OC$_{12}$H$_{25}$)** (3.56 g, 3.00 mmol), **3** (2.67 g, 12.03 mmol), Pd(PPh$_3$)$_4$ (0.17 g, 0.15 mmol), toluene (140 mL) and Na_2CO_3 (2 M) (15.00 mL, 30.07 mmol) was carefully degassed and afterward refluxed with vigorous stirring for 24 h. Separation of the organic layer, filtration, and evaporation under reduced pressure produced **4(4OC$_{12}$H$_{25}$)** as a grayish solid. Yield 3.73 g (90%).^{1}H NMR ($CDCl_3$): 0.88 (t, 12H, C*H*$_3$), 1.26−1.38 (m, 64H, CH$_3$(C*H*$_2$)$_8$), 1.43 (m, 8H, CH$_3$(CH$_2$)$_8$C*H*$_2$), 1.5−2 (three m, 12H, THP−C*H*$_2$), 1.74 (m, 8H, CH$_3$(CH$_2$)$_8$-CH$_2$C*H*$_2$), 3.64 (m, 2H, THP−OC*H*$_2$CH$_2$), 3.86 (t, 8H, CH$_2$C*H*$_2$O), 3.92 (m, 2H, THP−OC*H*$_2$CH$_2$), 4.93 (s, 4H, ArC*H*$_2$O), 5.46 (t, 2H, THP−OC*H*O), 6.35 (t, 2H, dendritic Ar−*H*), 6.45 (d, 4H, dendritic Ar−*H*), 7.03 (s, 2H, Ar−*H*), 7.08 (d, 4H, THPO−Ar−*H*), 7.54 (d, 4H, *H*−Ar−Ar). ^{13}C NMR ($CDCl_3$): 14.53 (*C*H$_3$), 19.21 (THP: CHCH$_2$*C*H$_2$), 23.1 (CH$_3$*C*H$_2$), 25.67 (THP: CH$_2$*C*H$_2$-CH$_2$O), 26.49 (CH$_3$CH$_2$*C*H$_2$), 29.69−30.1 (CH$_3$CH$_2$CH$_2$(*C*H$_2$)$_7$), 30.83 (THP: CH$_2$*C*H$_2$CHO), 32.33 (CH$_3$CH$_2$CH$_2$(CH$_2$)$_7$*C*H$_2$), 62.40 (THP: CH$_2$*C*H$_2$O), 68.44 (CH$_2$*C*H$_2$O), 71.91 (Ar*C*H$_2$O), 96.74 (THP: ArO−*C*HO), 101.22 (OC*C*HCO), 105.42 (OC*C*H-CCH$_2$O), 116.39 (THPOC*C*HCHCAr), 117.29 (ArC*C*HCO), 130.93−131.91 (Ar*C*CAr, ArC*C*Ar, ArC*C*HCHCOTHP), 140.05 (CH*C*CH$_2$O), 150.55 (O*C*CHCAr), 156.69 (THPO*C*CH), 160.73 (CH*C*OCH$_2$CH$_2$).

2′,5′-Di[3,5-bis(3,5-bis(dodecyloxy)benzyloxy)benzyloxy]-*p*-triphenylene-4′,4″-di(tetrahydropyranyloxy)-(4(8*OC$_{12}$H$_{25}$*)). A degassed mixture of **2(8OC$_{12}$H$_{25}$)** (3.00 g, 12.80 mmol), **3** (1.14 g, 5.14 mmol), PdCl$_2$(dppf) (0.0563 g, 0.0770 mmol), THF (80 mL), and NaOH (3 M) (51.20 mL, 15.36 mmol) was heated under reflux with vigorous stirring for 48 h. The organic layer was separated and filtrated, and the solvent was removed under reduced pressure. The product thus obtained was stirred with methanol, filtrated, and dried under vacuum. Yield 2.30 g (70%). ^{1}H NMR ($CDCl_3$): 0.87 (t, 24H, C*H*$_3$), 1.25−1.38 (m, 128H, CH$_3$(C*H*$_2$)$_8$), 1.43 (m, 16H, CH$_3$(CH$_2$)$_8$C*H*$_2$), 1.5−2 (three m, 12H, THP−C*H*$_2$), 1.76 (m, 16H, CH$_3$(CH$_2$)$_8$CH$_2$C*H*$_2$), 3.54 (m, 2H, THP−OC*H*$_2$CH$_2$), 3.83 (m, 2H, THP−OC*H*$_2$CH$_2$), 3.93 (t, 16H, CH$_2$C*H*$_2$O), 4.85 (s, 8H, ArC*H*$_2$O), 4.96 (s, 4H, ArC*H*$_2$O), 5.36 (t, 2H, THP−OC*H*O), 6.39 (t, 4H, dendritic Ar−*H*), 6.50 (t, 2H, dendritic Ar−*H*), 6.53 (d, 8H, dendritic Ar−*H*), 6.57 (d, 4H, dendritic Ar−*H*), 7.05 (s, 2H, Ar−*H*), 7.1 (d, 4H, THPO−Ar−*H*), 7.57 (d, 4H, *H*−Ar−Ar). ^{13}C NMR ($CDCl_3$): 14.52 (*C*H$_3$), 20.60 (THP: CHCH$_2$*C*H$_2$), 23.09 (CH$_3$*C*H$_2$), 25.64 (THP: CH$_2$*C*H$_2$CH$_2$O), 26.45 (CH$_3$CH$_2$-*C*H$_2$), 29.31−30.07 (CH$_3$CH$_2$CH$_2$(*C*H$_2$)$_7$), 31.10 (THP: CH$_2$*C*H$_2$-CHO), 32.32 (CH$_3$CH$_2$CH$_2$(CH$_2$)$_7$*C*H$_2$), 64.23 (THP: CH$_2$*C*H$_2$O), 68.48 (Ar*C*H$_2$O), 68.63 (CH$_2$*C*H$_2$O), 70.32 (Ar*C*H$_2$O), 95.08 (THP: ArO-*C*HO), 101.03 (OC*C*HCO), 101.22 (OC*C*HCO), 105.90 (OC*C*HCCH$_2$O), 106.22 (OC*C*HCCH$_2$O), 115.44 (THPOC-*C*HCHCAr), 116.39 (ArC*C*HCO), 130.80−131.24 (Ar*C*CAr, ArC*C*Ar, ArC*C*HCHCOTHP), 139.61 (CH*C*CH$_2$O), 140.25 (CH*C*CH$_2$O), 150.62 (O*C*CHCAr), 155.57 (THPO*C*CH), 160.35 (CH*C*OCH$_2$Ar), 160.81 (CH*C*OCH$_2$CH$_2$).

2′,5′-Di[3,5-bis(dodecyloxy)benzyloxy]-*p*-triphenylene-4′,4″-diol (5(4*OC$_{12}$H$_{25}$*)). Camphorosulfonic acid (CSA) (6.30 g, 27.12 mmol) was added to a solution of **4(4OC$_{12}$H$_{25}$)** (3.73 g, 2.70 mmol) in THF (50 mL) and MeOH (3 mL), and the mixture was stirred at room temperature for 18 h. Precipitation with MeOH, filtration, and washing with *n*-hexane afforded a white solid, **5(4OC$_{12}$H$_{25}$)**. Yield (75%). Anal. Calcd for C$_{80}$H$_{120}$O$_8$ (1210): C, 79.34; H, 10.08. Found: C, 78.93; H, 10.21. ^{1}H NMR ($CDCl_3$): 0.88 (t, 12H, C*H*$_3$), 1.26−1.38 (m, 64H, CH$_3$(C*H*$_2$)$_8$), 1.4 (m, 8H, CH$_3$(CH$_2$)$_8$C*H*$_2$), 1.74 (m, 8H, CH$_3$(CH$_2$)$_8$CH$_2$C*H*$_2$), 3.86 (t, 8H, CH$_2$C*H*$_2$O), 4.93 (s, 4H, ArC*H*$_2$O), 6.35 (t, 2H, dendritic Ar−*H*), 6.43 (d, 4H, dendritic Ar−*H*), 6.86 (d, 4H, HO−Ar−*H*), 7.01 (s, 2H, Ar−*H*), 7.50 (d, 4H, *H*−Ar−Ar). ^{13}C NMR ($CDCl_3$): 14.07 (*C*H$_3$), 22.65 (CH$_3$*C*H$_2$), 26.05 (CH$_3$CH$_2$*C*H$_2$), 29.27−29.65 (CH$_3$CH$_2$CH$_2$(*C*H$_2$)$_7$), 31.89 (CH$_3$CH$_2$CH$_2$(CH$_2$)$_7$*C*H$_2$), 68.07 (CH$_2$*C*H$_2$O), 71.67 (Ar*C*H$_2$O), 100.92 (OC*C*HCO), 105.12 (OC*C*HCCH$_2$O), 115.11 (HOC*C*H-CHCAr), 117.06 (ArC*C*HCO), 129.78−130.67 (Ar*C*CAr, ArC*C*Ar, ArC*C*HCHCOH), 139.75 (CH*C*CH$_2$O), 150.26 (O*C*CHCAr), 155.99 (HO*C*CH), 160.4 (CH*C*OCH$_2$CH$_2$).

2′,5′-Di[3,5-bis(3,5-bis(dodecyloxy)benzyloxy)benzyloxy]-*p*-triphenylene-4′,4″-diol (5(8*OC$_{12}$H$_{25}$*)). CSA (2.10 g, 9.04 mmol) was added to a solution of **4(8OC$_{12}$H$_{25}$)** (2.30 g, 0.90 mmol) in THF (40 mL) and MeOH (2 mL), and the mixture was stirred at room temperature for 18 h. Evaporation of the mother liquid under vacuum, stirring with MeOH, filtration, and washing with *n*-hexane afforded **5(8OC$_{12}$H$_{25}$)** as a grayish solid. Yield 1.29 g (60%). Anal. Calcd for C$_{156}$H$_{242}$O$_{16}$ (2370): C, 78.99; H, 10.21. Found: C, 78.7; H, 10.5. ^{1}H NMR ($CDCl_3$): 0.88 (t, 24H, C*H*$_3$), 1.26−1.39 (m, 128H, CH$_3$(C*H*$_2$)$_8$), 1.44 (m, 16H, CH$_3$(CH$_2$)$_8$C*H*$_2$), 1.78 (m, 16H, CH$_3$(CH$_2$)$_8$CH$_2$C*H*$_2$), 3.95 (t, 16H, CH$_2$C*H*$_2$O), 4.89 (s, 8H, ArC*H*$_2$O), 4.95 (s, 4H, ArC*H*$_2$O), 6.42 (t, 4H, dendritic Ar−*H*), 6.50 (t, 2H, dendritic Ar−*H*), 6.55 (d, 4H, dendritic Ar−*H*), 6.57 (d, 8H, dendritic Ar−*H*), 6.9 (d, 4H, HO−Ar−*H*), 7.05 (s, 2H, Ar−*H*), 7.51 (d, 4H, *H*−Ar−Ar). ^{13}C NMR ($CDCl_3$): 14.54 (*C*H$_3$), 23.1 (CH$_3$*C*H$_2$), 26.45 (CH$_3$CH$_2$*C*H$_2$), 29.6−30.08 (CH$_3$CH$_2$CH$_2$(*C*H$_2$)$_7$), 32.33 (CH$_3$CH$_2$CH$_2$(CH$_2$)$_7$*C*H$_2$), 68.61 (CH$_2$*C*H$_2$O), 70.32 (Ar*C*H$_2$O), 71.8 (Ar*C*H$_2$O), 101.02 (OC*C*HCO), 101.1 (OC*C*HCO), 106.22 (OC*C*HCCH$_2$O), 106.3 (OC*C*HCCH$_2$O), 115 (HOC*C*HCHCAr), 117 (ArC*C*HCO), 131.22−131.37 (Ar*C*CAr, ArC*C*Ar, ArC*C*HCHCOH), 139.58 (CH*C*CH$_2$O), 140 (CH*C*CH$_2$O), 150.5 (O*C*CHCAr), 160.32 (HO*C*CH), 160.79 (CH*C*OCH$_2$CH$_2$), 160.9 (CH*C*OCH$_2$Ar).

General Polymerization Procedure. A carefully degassed mixture of diol (1.0 mmol), α,*ω*-aliphatic dibromide (1.0 mmol), TBAH (0.4 mmol), *o*-DCB (5 mL), and NaOH (10 N) (5 mL) was vigorously stirred at 120 °C under a continuous stream of argon: **PETH-4OC$_{12}$H$_{25}$-*x***, 2−4 days; **PETH-8OC$_{12}$H$_{25}$-*x***, 4−8 days. The polymer thus formed was dissolved in $CHCl_3$ and precipitated in a 10-fold amount of methanol. Filtration, redissolvance in $CHCl_3$, and a second filtration afforded the salt-clean desired polymeric sample as white foam after reprecipitation in methanol or as a self-standing film after casting.

PETH-4OC$_{12}$H$_{25}$-*x*=12. A carefully degassed mixture of diol **5(4OC$_{12}$H$_{25}$)** (0.500 g, 0.413 mmol), α,*ω*-aliphatic dibromide *x* = 12 (0.136 g, 0.413 mmol), TBAH (0.056 g, 0.165 mol), *o*-dichlrobenzene (*o*-DCB) (1.8 mL), and NaOH (10 N) (1.8 mL) was vigorously stirred at 120 °C under a continuous stream of argon for 3 days. The polymer thus formed was dissolved in $CHCl_3$ and precipitated in a 10-fold amount of methanol. Filtration, redissolvance in $CHCl_3$, and a second filtration afforded the salt-free polymeric sample as white foam after reprecipitation in methanol or as a self-standing film after casting. Yield 0.60 g (94%) (Table 1, entry 1). ^{1}H NMR ($CDCl_3$): 0.79 (t, 12H, C*H*$_3$), 0.94−1.31 (two broad, 88H, CH$_3$(C*H*$_2$)$_9$ and CH$_2$(C*H*$_2$)$_8$CH$_2$), 1.63 (t, 8H, CH$_3$(CH$_2$)$_9$C*H*$_2$), 1.72 (broad, 4H, C*H*$_2$(CH$_2$)$_8$C*H*$_2$), 3.76 (t, 8H, CH$_2$C*H*$_2$O), 3.89 (broad, 4H, OC*H*$_2$CH$_2$(CH$_2$)$_8$CH$_2$C*H*$_2$O), 4.84 (s, 4H, ArC*H*$_2$O), 6.25 (s, 2H, dendritic Ar−*H*), 6.35 (s, 4H, dendritic Ar−*H*), 6.84 (d, 4H, CH$_2$O−Ar−*H*), 6.93 (s, 2H, Ar−*H*), 7.45 (d, 4H, *H*−Ar−Ar). ^{13}C NMR ($CDCl_3$): 14.54 (*C*H$_3$), 23.1 (CH$_3$*C*H$_2$), 26.48 (CH$_3$CH$_2$*C*H$_2$), 26.6 (OCH$_2$(CH$_2$)$_4$(*C*H$_2$)$_2$), 29.68−30.1 (CH$_3$-CH$_2$CH$_2$(*C*H$_2$)$_7$ and OCH$_2$(*C*H$_2$)$_4$(CH$_2$)$_2$), 32.33 (CH$_3$CH$_2$CH$_2$-(CH$_2$)$_7$*C*H$_2$), 68.41 (CH$_2$*C*H$_2$O), 71.91 (Ar*C*H$_2$O), 101.19 (OC*C*HCO), 105.39 (OC*C*HCCH$_2$O), 114.38 (OC*C*HCHCAr), 117.23 (ArC*C*HCO), 130.8−131.03 (Ar*C*CAr, ArC*C*Ar, ArC-*C*HCHCO), 140.06 (CH*C*CH$_2$O), 150.55 (O*C*CHCAr), 158.75 (O*C*CHCH), 160.7 (CH*C*OCH$_2$CH$_2$).

PETH-8OC$_{12}$H$_{25}$-*x*=12. A carefully degassed mixture of diol **5(8OC$_{12}$H$_{25}$)** (0.200 g, 0.084 mmol), α,*ω*-aliphatic dibromide *x* = 12 (0.027 g, 0.084 mmol), TBAH (0.012 g, 0.035 mmol), *o*-DCB (0.4 mL), and NaOH (10 N) (0.4 mL) was vigorously stirred at 120 °C under a continuous stream of argon for 8 days. The polymer thus formed was dissolved in $CHCl_3$ and precipitated in a 10-fold amount of methanol. Filtration, redissolvance in $CHCl_3$, and a second filtration afforded the

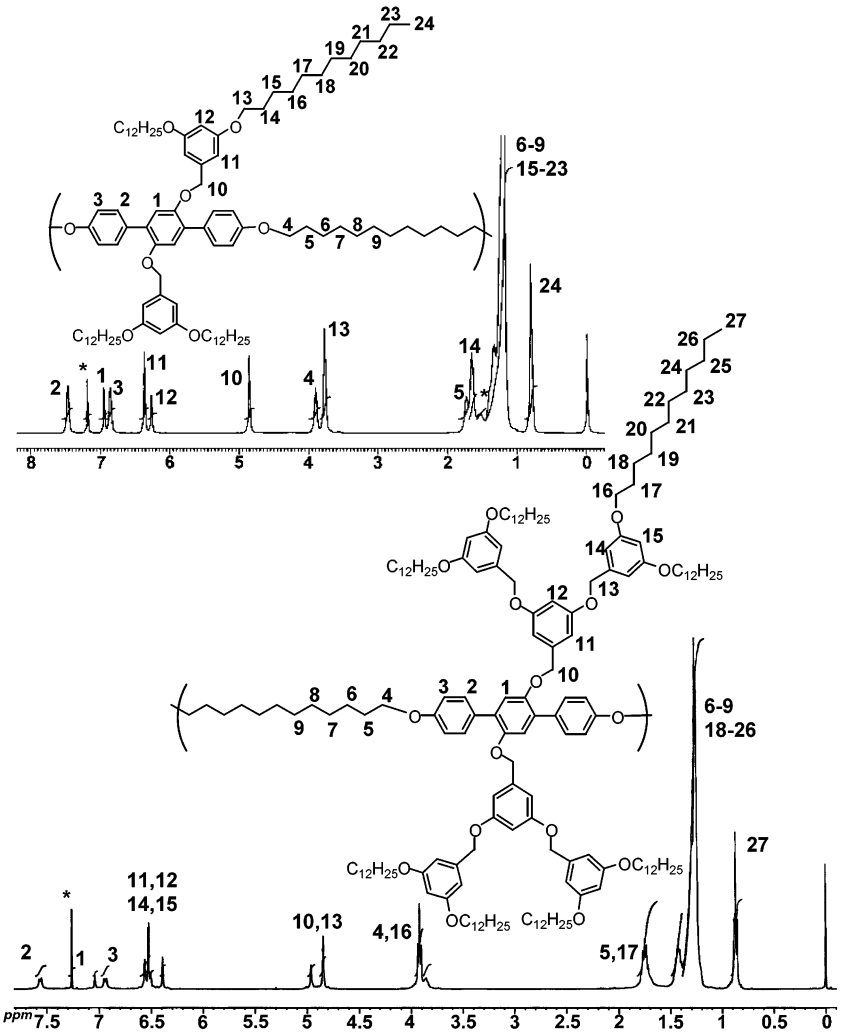

Figure 1. ^{1}H NMR spectra of **PETH-4OC$_{12}$H$_{25}$-*x*=12** (inset) and of **PETH-8OC$_{12}$H$_{25}$-*x*=12**.

salt-free polymeric sample as white foam after reprecipitation in methanol or as a self-standing film after casting. Yield 0.20 g (88%) (Table 1, entry 6). ^{1}H NMR ($CDCl_3$): 0.87 (t, 24H, C*H*$_3$), 1.26−1.44 (two broad, 160H, CH$_3$(C*H*$_2$)$_9$ and CH$_2$(C*H*$_2$)$_8$CH$_2$), 1.72−1.79 (two broad, 20H, CH$_3$(CH$_2$)$_9$C*H*$_2$ and C*H*$_2$(CH$_2$)$_8$C*H*$_2$), 3.86 (broad, 4H, OC*H*$_2$CH$_2$(CH$_2$)$_8$CH$_2$C*H*$_2$O), 3.92 (t, 16H, CH$_2$C*H*$_2$O), 4.85 (s, 8H, ArC*H*$_2$O), 4.97 (s, 4H, ArC*H*$_2$O), 6.4 (s, 4H, dendritic Ar−*H*), 6.49 (s, 2H, dendritic Ar−*H*), 6.53 (d, 8H, dendritic Ar−*H*), 6.57 (s, 4H, dendritic Ar−*H*), 6.94 (d, 4H, CH$_2$O−Ar−*H*), 7.05 (s, 2H, Ar−*H*), 7.56 (d, 4H, *H*−Ar−Ar). ^{13}C NMR ($CDCl_3$): 14.4 (*C*H$_3$), 23.08 (CH$_3$*C*H$_2$), 26.45 (CH$_3$CH$_2$*C*H$_2$ and OCH$_2$(CH$_2$)$_4$(*C*H$_2$)$_2$), 29.67−29.97 (CH$_3$-CH$_2$CH$_2$(*C*H$_2$)$_7$ and OCH$_2$(*C*H$_2$)$_4$(CH$_2$)$_2$), 32.26 (CH$_3$CH$_2$*C*H$_2$-(CH$_2$)$_7$CH$_2$), 68.52 (CH$_2$*C*H$_2$O), 70.6 (Ar*C*H$_2$O), 72.06 (Ar*C*H$_2$O), 101.42 (O*C*CHCO), 102.23 (O*C*CHCO), 106.1 (O*C*CHCCH$_2$O), 106.29 (O*C*CHCCH$_2$O), 114.5 (O*C*CHCHCAr), 117.45 (ArC-*C*HCO), 130.82−131.22 (Ar*C*CAr, ArC*C*Ar, ArC*C*HCHCO), 139.45 (CH*C*CH$_2$O), 140.3 (CH*C*CH$_2$O), 150.76 (O*C*CHCAr), 158.9 (O*C*CHCH), 160.47 (CH*C*OCH$_2$Ar), 160.95 (CH*C*OCH$_2$-CH$_2$).

Results and Discussion

Monomer and Polymer Syntheses. In light of some of our previous findings,[21] we anticipated that aromatic−aliphatic dendronized polyethers bearing two alkoxy functionalized side dendrons onto every repeating unit would provide soluble, high molecular weight, film forming materials with interesting bulk properties. Furthermore, we were interested in exploiting their solid-state conformational behavior and determining whether this kind of dendrons would dominate any organizational features in the final polymeric materials.

In general, the alkoxy dendritic fragments employed up to now in the literature were usually 3,4,5-, 3,4-, or 4-substituted ones. A combination of these kinds of dendrons with the 3,5-disubstituted benzyl ethers of the Fréchet type was also made in an effort to discriminate variations between the different dendritic structures.[23] Also, in this case the flexible chains led to a similar arrangement of the dendrons like in the former cases. However, an investigation of dendronized polymers bearing dendrons of the Fréchet-type periphery decorated with lengthy alkoxy groups, rising from polymerization conditions other than chain-growth ones, has been only once attempted so far, but their investigation referred strictly to the optical properties of the conjugated main polymeric backbones.[15]

Following a macromonomer approach that has proven to be extremely efficient for the syntheses of oligophenylene-dendronized macromonomers, we originally prepared, using the convergent methodology,[24] aromatic dibromides bearing side dendrons[10] of the first or second generation, respectively, decorated with dodecyloxy periphery end groups (Scheme 1). The dibromides **2(G$_1$) = 2(4OC$_{12}$H$_{25}$)** and **2(G$_2$) = 2(8OC$_{12}$H$_{25}$)** were then coupled with the tetrahydropyran (THP) protected hy-

droxyl phenylboronic acid (**3**)[21] under palladium-mediated Suzuki coupling conditions.[25] Removing the THP end protecting groups in a mild acidic environment finally produced the hydroxy end functionalized terphenyl diols of the first or second generation carrying the two side dendrons in their middle phenylene ring, **5(4OC$_{12}$H$_{25}$)** and **5(8OC$_{12}$H$_{25}$)**, respectively. These final macromonomer diols were subsequently polymerized under phase transfer conditions[26] with α,ω-aliphatic dibromides of various lengths (Scheme 2). High molecular weight polyethers were obtained in most cases as depicted from their GPC results using a PS standard calibration (Table 1), with good solubilities in common chlorinated solvents for both the first and second generation polyethers. The first generation alkoxy-functionalized polyethers, **PETH-4OC$_{12}$H$_{25}$-*x***, are more soluble in milder solvents like chloroform than the analogous ones bearing side dendrons of the Fréchet type.[21] However, the true molecular weights of these polymeric materials should be higher by at least a factor of 2, since GPC determination using PS standards underestimates their actual molecular characteristics.[3,9,21,27] Their ^{1}H and ^{13}C NMR characterization is in full agreement with the proposed structures, and moreover no end groups were detectable throughout the polymeric main chains proving the efficiency of the polymerization conditions employed (Figure 1).

Thermal and Solid-State Properties. The initial characterization of polyethers bearing first generation dendrons **PETH-4OC$_{12}$H$_{25}$-*x*** has been performed by means of the differential scanning calorimetry (DSC). Parts a and b of Figure 2 show the representative thermograms recorded during heating and cooling, respectively. For comparison, the DSC thermogram of the macromonomer diol **5(4OC$_{12}$H$_{25}$)** is shown in Figure 2d. Intense melting (T_m) and crystallization (T_c) transitions (see Table 2) were observed for all polymeric samples, but no glass transition temperatures were noticeable for any of them. On the other hand, diol **5(4OC$_{12}$H$_{25}$)** exhibited two transitions (Figure 2d) observed both during heating and cooling, indicating a mesophase in the temperature range between ~60 and ~120 °C, which separates the crystalline and isotropic states situated at lower and higher temperatures, respectively. Whereas, in the diol, the melting or crystallization DSC peaks are sharp and nearly symmetric, the polymers' endothermic transitions are highly asymmetric and considerably broadened on the low-temperature side. This kind of behavior is characteristic for systems which show a partial melting consisting of dismounting or rearranging structures of various thermal stability. Most of the thermograms presented in Figure 2a indicate such premelting or structural reorganization taking place at temperatures extending much below the main melting peak. This effect extends to temperatures below the room temperature, which means that samples kept at normal conditions have a fraction of material, which could crystallize when cooled down or when conditions are created for formation of more thermally stable structures.

Taking this into account, the same polymeric samples were also examined, using the same testing conditions after keeping them for three months at room temperature in order to determine possible formation of secondary structures due to additional slow relaxations. For the samples aged in the above-described way (Figure 2c), two well-resolved endothermic peaks were seen, one at the lower temperature region (T_{m_a}) and a second one at the region of the initially observed main endothermic transitions (T_m).

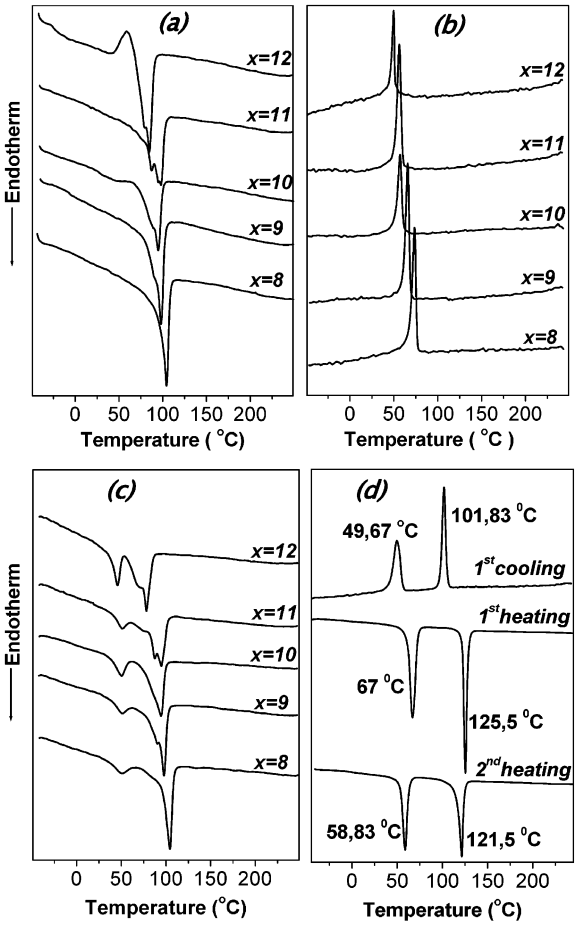

Figure 2. DSC thermograms of **PETH-4OC$_{12}$H$_{25}$-*x*** samples: (a) second heating runs, (b) first cooling runs, (c) after aging of the samples at room temperature for 3 months, first heating run, and (d) of the corresponding macromonomer diol **5-(4OC$_{12}$H$_{25}$)**.

The melting (T_m) and crystallization (T_c) temperatures are dependent on the number of methylene units (x) along the main-chain flexible spacer, as depicted in Figure 3. On the other hand, the new transition T_{m_a}, which appears just above the temperature of sample storage, seems to be independent of x. The fact that this additional melting observed only after a kind of aging does not depend on x indicates that it should be related to melting of material fractions which became ordered in a secondary crystallization process requiring a lot of time and creating structures stable just at and slightly above the samples' storage temperature.

The main transitions (T_m, T_c) were also observed using polarized optical microscopy (POM) where the growth of spherulites throughout the polymeric samples was detected during cooling from the isotropic melt (2 °C/min). This indicated that the structure formation in the polymers goes by nucleation and growth, which usually can be strongly influenced by cooling rates or temperature of an isothermal process. Employing small-angle light scattering (SALS)[22] under the same conditions as for the POM experiments, scattering patterns characteristic for the spherulites were observed under crossed (Hv) polarizers. The size of the spherulites was estimated to vary in the range between 3 and 9 μm with a tendency of decreasing spherulites' size (higher nucle-

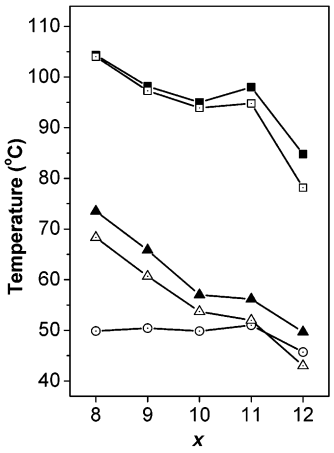

Figure 3. Variation of the transition temperatures as determined from the DSC experiments (Table 2) vs the number of methylene units along the main polymeric chain *x*, for **PETH-4OC$_{12}$H$_{25}$-*x*** samples. Second heating: T_m, ■; T_c, ▲. After aging at room temperature for 3 months: T_{m_a}, ○; T_m, □; T_c, △.

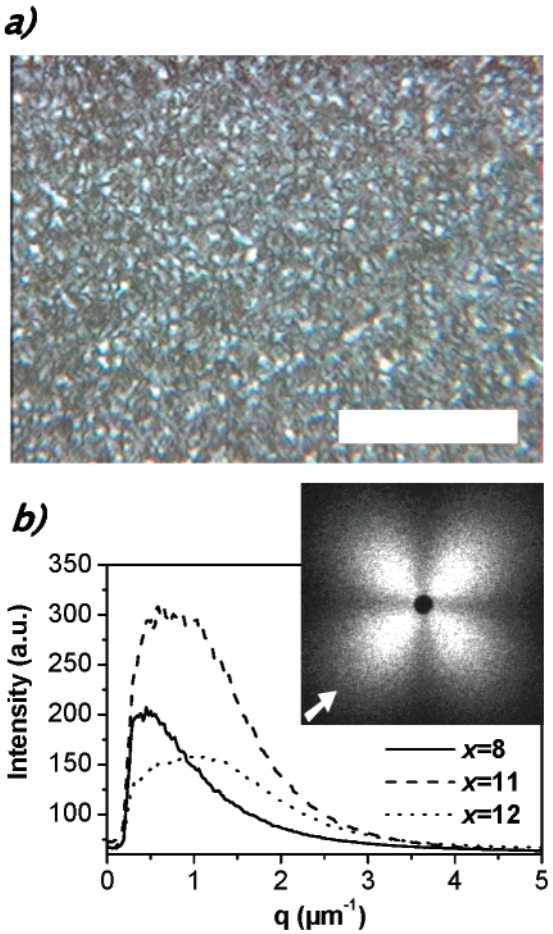

Figure 4. POM picture (a) and the SALS pattern (b) corresponding to **PETH-4OC$_{12}$H$_{25}$-*x*=11** at room temperature. The white bar in (a) represents a size of 100 μm. The intensity distributions in (b) are recorded at 45° with respect to polarization directions in the Hv pattern.

ation density) with increasing spacer length *x*. An example of the Hv scattering pattern and some intensity distributions allowing determination of spherulites' size are presented in Figure 4.

For polyethers bearing second generation alkoxy side dendrons, a representative DSC thermogram is given in Figure 5a for **PETH-8OC$_{12}$H$_{25}$-*x*=12** together with

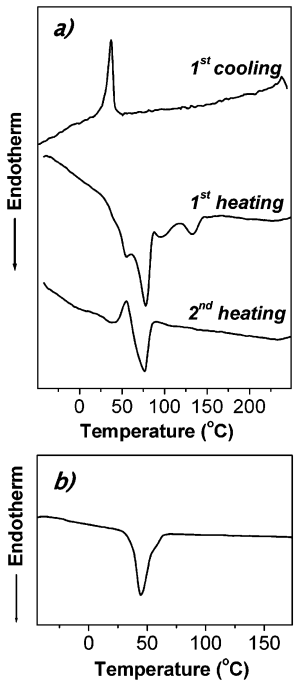

Figure 5. DSC thermograms of (a) **PETH-8OC$_{12}$H$_{25}$-*x*=12** first and second heating cycle and first cooling cycle and (b) macromonomer diol **5(8OC$_{12}$H$_{25}$)**.

the thermogram of the corresponding macromonomer diol **5(8OC$_{12}$H$_{25}$)** (Figure 5b). A complex first heating curve was obtained for **PETH-8OC$_{12}$H$_{25}$-*x*=12** while only one exothermic peak was observed during cooling followed by a much simpler second heating curve. The macromonomer diol **5(8OC$_{12}$H$_{25}$)** showed only one endothermic transition during the first heating with no crystallization or melting transitions during the following cycles. After remaining at room temperature for some days the same diol sample again presented only one first endothermic peak, revealing a difficulty toward crystallization.

Dynamic mechanical measurements for polymers **PETH-4OC$_{12}$H$_{25}$-*x*** were performed for the evaluation of their properties under shear deformation in a broad temperature range. Temperature sweep tests were conducted during both heating and cooling of the polymeric samples. Figure 6 shows the results obtained during cooling for samples with various spacer lengths (Figure 6a) and during cooling and heating for one sample with $x = 11$ (Figure 6b). As expected, pronounced changes of the storage and loss shear moduli (G' and G'', respectively) were observed during crystallization or melting of the polymers. These changes demonstrate the transition between the polymers' solid and liquid like states. From the above experiments the T_m and T_c temperatures were also determined which revealed the same dependencies on *x* as was initially detected during their DSC tests (see Figure 3). Another interesting feature in the G' and G'' curves is the existence of small changes in their slopes in the temperature region at about 50 °C, probably indicating an onset of mobility related to partial melting of the secondary crystallized material, in agreement with the observations made by means of DSC for the aged samples.

Polyethers carrying either first **(4OC$_{12}$H$_{25}$)** or second **(8OC$_{12}$H$_{25}$)** generation side dendrons have shown an interesting property of forming stable, self-standing films after melt-pressing or casting from chloroform

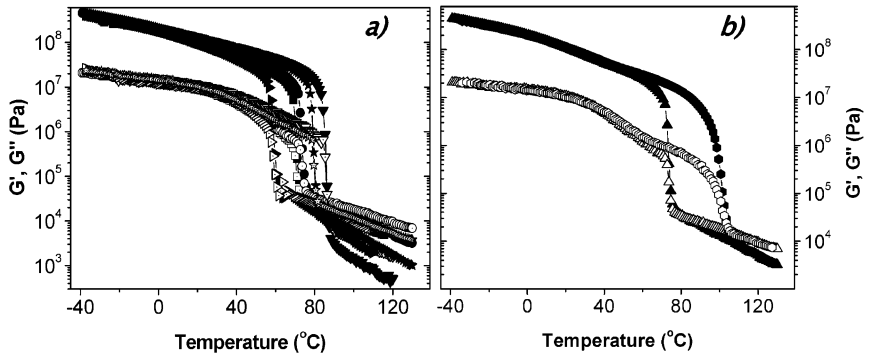

Figure 6. Temperature dependencies of the real (G', filled symbols) and imaginary (G'', open symbols) parts of the complex shear modulus for PETH-4$OC_{12}H_{25}$-x samples [x = 12 tilted ▲, △; x = 11 ●, ○; x = 10 ■, □; x = 9 ★, ☆; x = 8 ▼, ▽] (a) during cooling from the melt and (b) during cooling (▲, △) and heating (●, ○) obtained for the **PETH-4OC$_{12}$H$_{25}$-x=11** sample.

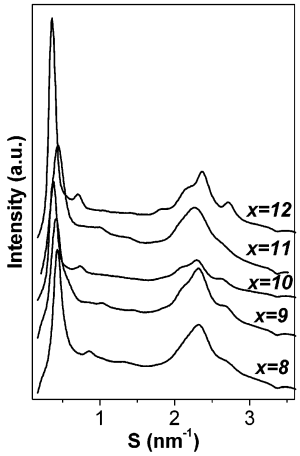

Figure 7. X-ray diffraction intensity distributions for **PETH-4OC$_{12}$H$_{25}$-x** samples in film form as casted from $CHCl_3$ solutions.

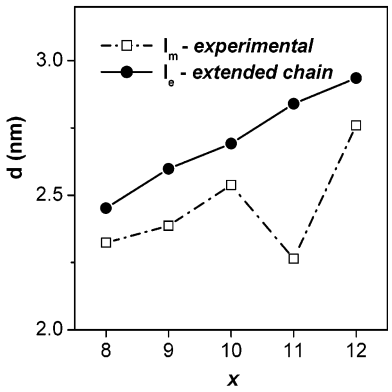

Figure 8. Distances corresponding to the first intensive peak in the diffraction from **PETH-4OC$_{12}$H$_{25}$-x** samples as a function of the number of repeating units in the flexible backbone spacer. For comparison, lengths of extended repeating units in the simulated backbones are shown.

solutions. These films were investigated employing wide-angle X-ray scattering (WAXS) at room temperature. The results indicate quite complex self-organization effects depending on both the parameters of the molecular structure and conditions of sample treatment. As an example, Figure 7 shows the scattered intensity distributions recorded for all **PETH-4OC$_{12}$H$_{25}$-x** samples in film form. The experiments were in this case performed with the X-ray beam perpendicular to the film surface. Intense diffraction peaks were detected in the small-angle region and were accompanied by weaker diffraction peaks and an amorphous halo in the wide-angle region. Distances corresponding to the intense small-angle diffraction have made impression to be correlated with the length of the flexible repeating unit in the polymeric backbone. In Figure 8, these distances are compared with the simulated dimensions of fully extended repeating units along the backbone (Chem 3D Ultra 7.0). For an even number of methylene units in the flexible backbone spacer, the experimentally detected distances nearly reach the extended ones. Polymers with an odd number of units in the spacer do not follow this tendency, however, an explanation of that requires further investigation. The assignment of the low-angle peak to the periodicity along the backbone was also supported by analysis of the 2D diffraction patterns recorded for samples oriented by drawing at temperatures close to their crystallization temperature. An example of such patterns can be viewed in parts a and b of Figure 9 for an as-drawn and annealed fiber of **PETH-4OC$_{12}$H$_{25}$-x=12**, respectively. Additionally, the intensity distributions recorded along the equatorial and meridional directions corresponding to the annealed sample are presented in Figure 9. These patterns indicate a clear ordering along the drawing direction, as well as in the perpendicular one. The meridional reflections correspond to the periodicity of the chains oriented along the drawing direction. In the annealed sample (Figure 9b), a large number of higher-order reflections indicate a high uniformity in the chain periodicity and related supramolecular structure. The equatorial reflections demonstrate the lateral ordering of the aligned and extended chains into a layered structure. Annealing of the oriented sample was performed at 50 °C, which is close to the polymers' crystallization temperature, leading to an improved order as illustrated in Figure 9b. Changes such as the development of more higher-order reflections in the meridional direction and the more or less loss of its wider-angle amorphous halo, while simultaneously changes of the preexisting diffractions from a linear to a more spherical shape, are clearly observed, pointing out a better molecular organization in the annealed sample.

Also, in the case of the second generation polymeric films, ordered structures were detected. An example of a diffraction pattern for polyether **PETH-8OC$_{12}$H$_{25}$-x=12** is given in Figure 10. The pattern was obtained from a drawn film with the drawing direction vertical. The diffraction also in this case indicates ordering both along the drawing direction and in the direction lateral with respect to the oriented polymeric chains. A comparison of correlation distances corresponding to the meridional and equatorial peaks revealed that ordering

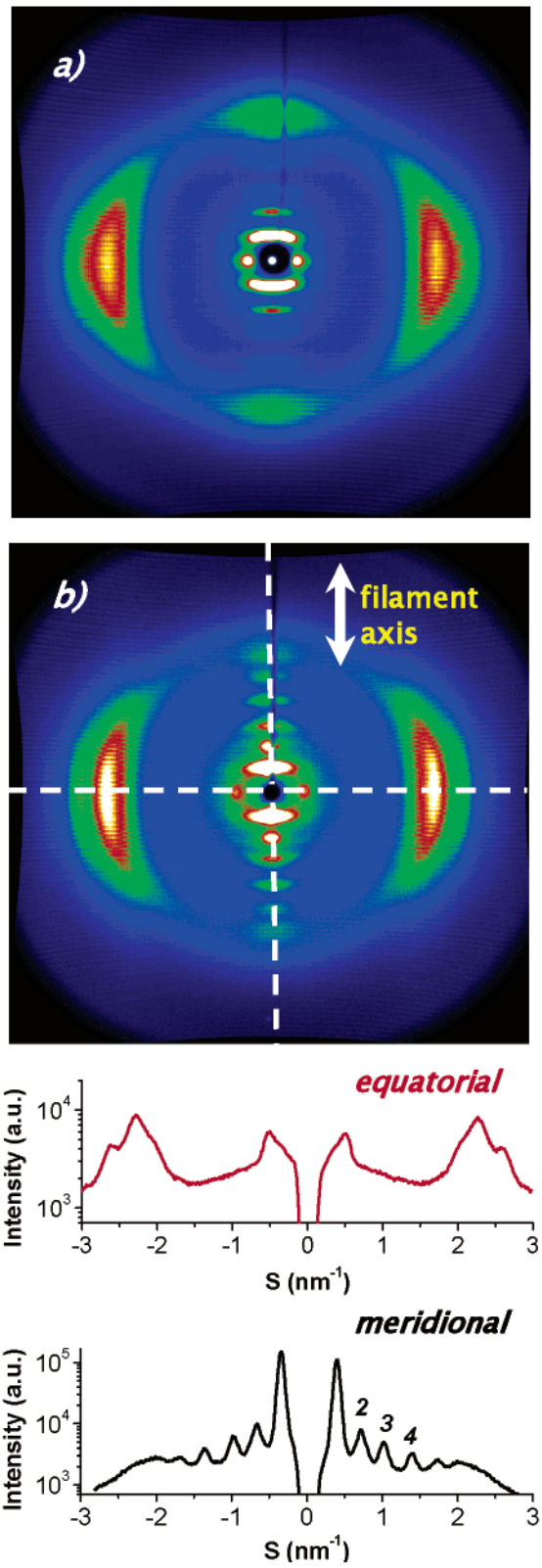

Figure 9. 2D X-ray diffraction pattern of an oriented sample of **PETH-4OC$_{12}$H$_{25}$-*x*=12** before (a) and after (b) annealing. Two intensity distributions measured along the equatorial and meridional directions in pattern (b) are shown. The directions are indicated in the pattern (b) by dashed horizontal and vertical lines, respectively. Positions of intensity maxima in the meridional intensity distribution satisfied the ratios indicated in the figure. For the discussion of this effect see the text.

along polymeric backbones has nearly the same periodicity as was observed for the first generation polymers

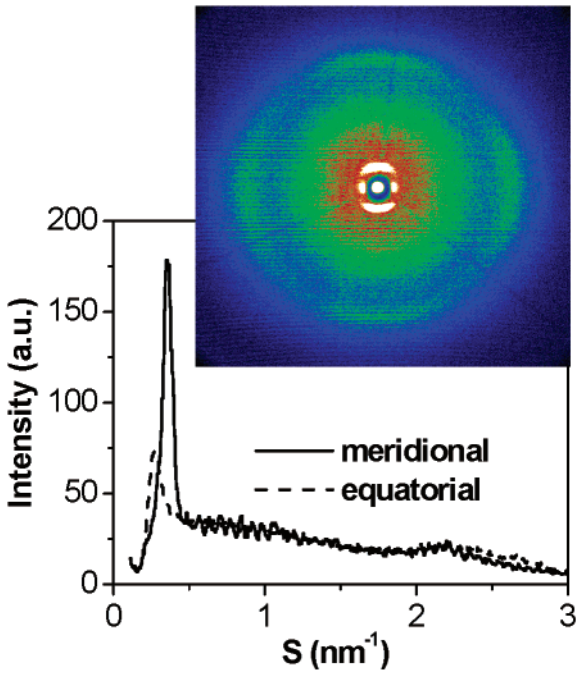

Figure 10. 2D X-ray diffraction pattern and corresponding equatorial and meridional intensity distributions of an oriented sample of **PETH-8OC$_{12}$H$_{25}$-*x*=12**.

with the same length of flexible spacer, but the distances indicated by the equatorial reflections became larger by a factor nearly reflecting an increase of the side groups molecular mass. This shows that, also in the case of polyethers with higher generation side dendrons, the backbones assume a nearly extended conformation, and their lateral ordering is controlled by the size of the side dendrons.

From the above results, even though a much detailed investigation is intended, some first conclusions over the organization of these dendronized polymeric materials can be extracted. A consideration concerning the structure in oriented filaments is based on a qualitative analysis of the diffractograms presented in Figure 9. We assume that the structure in such oriented states is controlled primarily by chain extension along the axes of the filaments but also by the mesogenic character of the terphenyl segments equidistantly distributed along the polymer backbones and by the packing possibilities of the complex units to a bulk material. To simplify further discussion, we map the studied molecular structures by the simple scheme of the generalized repeating unit as shown in Figure 11. Joining such units to a polymer results in a structure presented schematically on the right-hand side of the figure. Such simplified polymers are used in Figure 12 to represent macromolecular arrangements, which could lead to the observed scattering patterns. Two most probable, in our opinion, local arrangements are presented. In one case (structure **A**, Figure 12), an assembly of well-extended polymer chains with backbones separated into layers and the mesogenic units forming a nematic 2D mesophase within the layers is considered. Such a structure contributes to scattering effects dependent on the orientation of the volume element with respect to the incident X-ray beam. We consider two characteristic situations leading to diffractions reflecting the main features of the structure. With the chains oriented vertically (*c* axis) and the X-ray beam nearly perpendicular to the backbone layers (*a* axis), the scattering

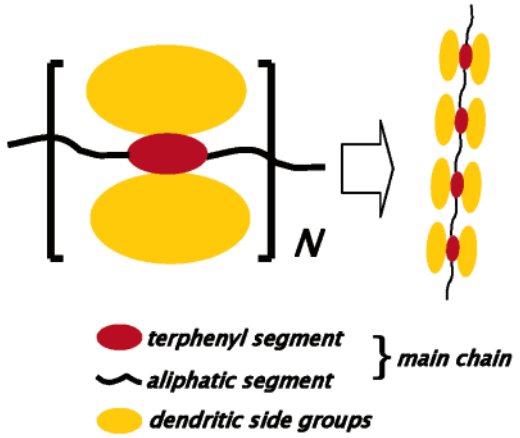

Figure 11. Schematic representation of the monomer and the polymer with distinctions only of the most important architectural units.

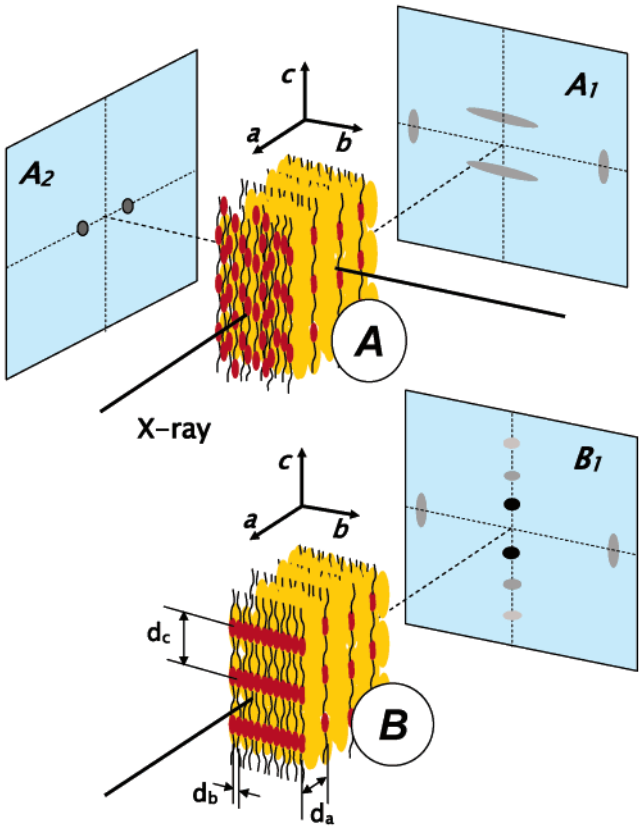

Figure 12. Schematic illustration of the two types of local order postulated for the drawn polymers and corresponding scattering effects dependent on the orientation of the structure with respect to the incident X-ray beam. The structures consist of the main-chain layers separated by the side groups (dendrons) and differ by the type of arrangement within the main-chain layers: A, nematic; B, smectic.

will reflect mainly the organization within these layers. In the considered case of nematic order, characteristic sets of meridional and equatorial reflections are expected (pattern $\mathbf{A_1}$) which should indicate periodicities along the backbone and in the transversal direction, respectively. Because of only single-chain correlations assumed, the meridional reflections have a specific shape (extended in the horizontal direction).[28] The equatorial spots are considered as indicating the backbone−backbone correlations within the layers. In the second case (structure **B**, Figure 12), a smectic-like order

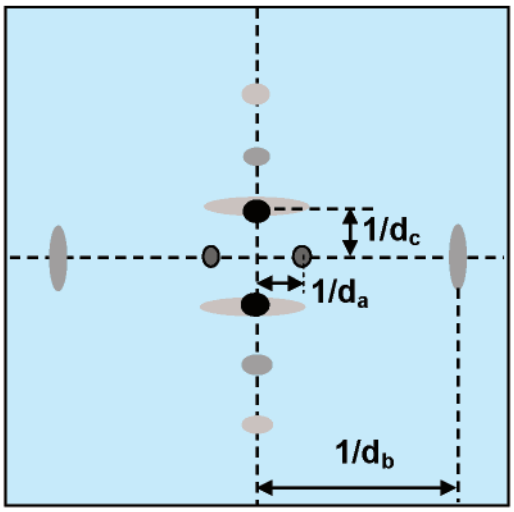

Figure 13. Schematic representation of the 2D fiber scattering pattern with contributions of effects related to both structures considered in Figure 12. The reflections containing information about the dimensions d_a, d_b, and d_c in the real space are indicated.

within the backbone layers is taken into account, for which the resulting scattering pattern ($\mathbf{B_1}$) exhibits a series of meridional spots which indicate the period of the correlations along the backbone. The number of higher-order reflections in this case can be correlated with extension of the order in the direction of the oriented chains and the horizontal width of the reflections with the extension of order in the transversal direction.

With the beam nearly parallel to the backbone layers (*b* axis), the diffraction pattern ($\mathbf{A_2}$) reflects the interlayer period in the form of the equatorial reflections. For both structures considered this effect is supposed to be similar. Again here, depending on the range and perfection of layered correlations, the number of higher-order equatorial reflections would be influenced. Lack of higher-order reflections means a short-range correlation only. For the layered structure considered, the interlayer spacing should be proportional to the size of the side groups (in this case dendrons) when the extension and constitution of the backbones remain constant. The fact that in these systems the proportionality is nearly preserved with the variation of dendrons' generations constitutes a strong argument for the layered structures in the studied materials.

The two cases of order presented in Figure 12 seem to appear exclusively or simultaneously in the studied samples, depending on the architectural details and on the thermal treatment. For example, the as-drawn sample (Figure 9a) can be considered as having the structure with the nematic order within the backbone layers (structure **A**, Figure 12) predominantly. Annealing of the drawn sample seems to involve a transformation of this structure to the smectic one (structure **B**, Figure 12). However, in the observed case (Figure 9b), the transformation is not complete so that the scattering pattern consists of contributions of the two types of order. A schematic representation of such a pattern is shown in Figure 13. It contains a superposition of all effects illustrated separately in Figure 12. The equatorial reflections in the small- and wide-angle range in this pattern reflect the interlayer and backbone−backbone correlation periods, respectively. They can be considered as not distinguishably similar in the two

postulated structures. In the meridional direction, the effects of periodicities along the backbones, different for the two discussed structures, overlap so that the shape and position of the small-angle reflection may not effectively fit to the higher-order reflections characteristic for the structure **B** (see Figure 12). Such a pattern is in our opinion in a good qualitative agreement with the one observed for the annealed polymer (Figure 9b). The assumed superposition of the scattering from the two structures explains the initially somewhat puzzling effect of discrepancy of the position of the first meridional intensity maximum from the sequence constituting ratios 1, 2, 3, etc., with the higher-order meridional intensity maxima which, on the other hand, starting form the second peak satisfy the ratios 2, 3, 4, etc. (see Figure 9).

According to the above arguments, a layered structure consisting of main polymeric backbones with the side dendritic moieties filling the space between neighboring layers is the most probable organizational pattern for these dendronized polyethers. The length of the flexible spacer in the backbone, distinguishing for these series, appears as a parameter that can introduce large changes in the final polymeric properties. Moreover, the structural motives observed here seem to be unique also in comparison with other SCDPs consisting of macromolecules having some analogous elements in their architectures. For example, they differ considerably from the bulk structures of Schlüter's dendronized polymers[3] for which the dendrons form cylindrical coatings around the backbones leading to amorphous assemblies of the flexible cylinders in bulk.[29] They also differ from densely substituted polyesters[30] or polyparaphenylenes,[31] in which despite the frequently observed well-developed layered structures, no comparable ordering along the backbones has been detected.

Moreover, it is worth noticing that when going from a flexible main polymeric backbone to a semirigid one, we obtained different organizational patterns than those so far reported for alkoxy functionalized dendronized polymeric materials, such as polystyrene. Actually, Percec's main-chain flexible polymers self-organize strictly due to the favorable arrangement of the side dendrons in LC phases, producing mostly hexagonal−columnar arrays.[16]

A more comprehensive investigation of the observed effects considering broader variation of the structural parameters and preparation conditions is now in progress, and the results will be presented elsewhere. However, these dendronized rigid−flexible polyethers considered here could constitute a new potential to modify architectural parameters and polymeric properties in the bulk state. This paper already shows that the complex balance of the rigidity and flexibility along the main polymeric backbones under packing requirements of the surrounding large side dendritic groups may lead to unusual supramolecular organizations, thus introducing interesting characteristics to the final polymeric materials.

Conclusions

Side-chain dendritic polyethers comprised of rigid−flexible main-chain polymeric backbones disubstituted by first or second generation dodecyloxy periphery decorated dendritic wedges are reported in this contribution. Using a well-established synthetic route toward such alternating dendronized polyethers allowed for high molecular weight, soluble polymers to be obtained with excellent film forming properties. These particular dendronized polyethers showed a high tendency toward self-organization, as indicated by the results of various experimental techniques (DSC, POM, SALS, and WAXS). Their bulk characteristics were also examined under shear deformation conditions, which provided information for their mechanical properties. The results indicated a relatively strong dependence of melting and crystallization temperatures on rather small variation of the polymeric structure, in particular by varying the number of methylene units along the main-chain flexible spacer. The polymers have shown an ability to form macroscopically well-oriented structures as indicated by means of X-ray diffraction. A layered structure consisting of main-chain polymeric backbones with the side dendritic moieties occupying the space in between can be concluded for all the examined systems with various parameters of the main-chain's and the side-dendrons' architectures affecting the final organizational characteristics. The LC type of ordering of the extended backbones within the main-chain layers is postulated and can be considered as nematic or smectic depending on details of the molecular parameters and thermal treatment.

Acknowledgment. The authors are indebted to Prof. G. Wegner (MPIP-Mainz) for helpful discussions and suggestions. This work was partially supported by the Marie-Curie-Training Site "Methods of Polymer Characterization" HPMT-CT-2000-00015 and by the Operational Programme for Education and Initial Vocational Training on "Polymer Science and Technology" 3.2a, 33H6, administered through the Ministry of Education in Greece.

References and Notes

(1) (a) Lehn, J. M. *Supramolecular Chemistry;* VCH: Weinheim, 1995. (b) Whitesides, G. M.; Mathias, J. P.; Seto, C. P. *Science* **1991**, *254*, 1312.

(2) (a) Newkome, G. R.; Moorefield, C. N.; Vögtle, F. *Dendrimers and Dendrons: Concepts, Syntheses, Applications;* Wiley-VCH: New York, 2001. (b) Fréchet, J. M. J.; Tomalia, D. A. *Dendrimers and other Dendritic Polymers*; Wiley-VCH: New York, 2001.

(3) Schlüter, D. A.; Rabe, J. P. *Angew. Chem., Int. Ed.* **2000**, *39*, 864.

(4) (a) Zeng, F.; Zimmerman, S. C. *Chem. Rev.* **1997**, *97*, 1681. (b) Vögtle, F. Dendrimers II, Architecture, Nanostructure and Supramolecular Chemistry. In *Top. Curr. Chem.* **2000**, *210*, 1. (c) Hawker, C. J. *Curr. Opin. Colloid Interface Sci.* **1999**, *4*, 117. (d) Gittins, P. J.; Twyman, L. J. *Supramol. Chem.* **2003**, *15*, 5.

(5) Percec, V.; Ahn, C.-H.; Ungar, G.; Yeardley, D. J. P.; Möller, M.; Sheiko, S. S. *Nature (London)* **1998**, *391*, 161.

(6) (a) Balagurusamy, V. S. K.; Ungar, G.; Percec, V.; Johansson, G. *J. Am. Chem. Soc.* **1997**, *119*, 1539. (b) Percec, V.; Ahn, C.-H.; Cho, W.-D.; Jamieson, A. M.; Kim, J.; Leman, T.; Schmidt, M.; Gerle, M.; Möller, M.; Prokhorova, S. A.; Sheiko, S. S.; Cheng, S. Z. D.; Zhang, A.; Ungar, G.; Yeardley, D. J. P. *J. Am. Chem. Soc.* **1998**, *120*, 8619. (c) Percec, V.; Cho, W.-D.; C.-H.; Ungar, G. *J. Am. Chem. Soc.* **2000**, *122*, 10273. (d) Percec, V.; Cho, W.-D.; Ungar, G.; Yeardley, D. J. P. *J. Am. Chem. Soc.* **2001**, *123*, 1302. (e) Percec, V.; Glodde, M.; Bera, T. K.; Miura, Y.; Shiyanovskaya, I.; Singer, K. D.; Balagurusamy, V. S. K.; Heiney, P. A.; Schnell, I.; Rapp, A.; Spiess, H.-W.; Hudson, S. D.; Duan, H. *Nature (London)* **2002**, *419*, 384. (f) Percec, V.; Bera, T. K.; Glodde, M.; Fu, Q.; Balagurusamy, V. S. K.; Heiney, P. A. *Chem.—Eur. J.* **2003**, *9*, 921.

(7) (a) Schenning, A.; Roman, C.; Weener, J.; Baars, M.; van der Gaast, S.; Meijer, E. *J. Am. Chem. Soc.* **1998**, *120*, 8199. (b) Suárez, M.; Lehn, J. M.; Zimmerman, S. C.; Skoulios, A.; Heinrich, B. *J. Am. Chem. Soc.* **1998**, *120*, 9526. (c) Bo, Z.;

Rabe, J. P.; Schlüter, D. A. *Angew. Chem., Int. Ed.* **1999**, *38*, 2370. (d) Gössl, I.; Shu, L.; Schlüter, A. D.; Rabe, J. P. *J. Am. Chem. Soc.* **2002**, *124*, 6860. (e) Felder, D.; Galliani, J.-L.; Guillon, D.; Heinrich, B.; Nicoud, J.-F.; Nierengarten, J.-F. *Angew. Chem., Int. Ed.* **2000**, *39*, 201. (f) Marcos, M.; Giménez, R.; Serrano, J. L.; Donnio, B.; Heinrich, B.; Guillon, D. *Chem.—Eur. J.* **2001**, *7*, 1006. (g) Saez, I. M.; Goodby, J. W.; Richardson, R. M. *Chem.—Eur. J.* **2001**, *7*, 2758. (h) Kimura, M.; Saito, Y.; Ohta, K.; Hanabusa, K.; Shirai, H.; Kobayashi, N. *J. Am. Chem. Soc.* **2002**, *124*, 5274.

(8) (a) Tschierske, C. *J. Mater. Chem.* **2001**, *11*, 2647. (b) Tschierske, C. *J. Mater. Chem.* **1998**, *8*, 1485. (c) Tschierske, C. *Annu. Rep. Prog. Chem., Sect. C: Phys. Chem.* **2001**, *97*, 191. (d) Bates, F. S.; Fredrickson, G. H. *Phys. Today* **1999**, 32. (e) Lee, M.; Cho, B.-K.; Ihn, K. J.; Lee, W.-K.; Oh, N.-K.; Zin, W.-C. *J. Am. Chem.* **2001**, *123*, 4647.

(9) Zhang, A.; Shu, L.; Bo, Z.; Schlüter, D. A. *Macromol. Chem. Phys.* **2003**, *204*, 328.

(10) Bo, Z.; Zhang, X.; Yi, X.; Yang, M.; Shen, J.; Ren, Y.; Xi, S. *Polym. Bull. (Berlin)* **1997**, *38*, 257.

(11) Representative examples can be found in: (a) Hudson, S. D.; Jung, H.-T.; Percec, V.; Cho, W.-D.; Johansson, G.; Ungar, G.; Balagurusamy, V. S. K. *Science* **1997**, *278*, 449. (b) Percec, V.; Cho, W.-D.; Mosier, P. E.; Ungar, G.; Yeardley, D. J. P. *J. Am. Chem. Soc.* **1998**, *120*, 11061. (c) Percec, V.; Ahn, C.-H.; Bera, T. K.; Ungar, G.; Yeardley, D. J. P. *Chem.—Eur. J.* **1999**, *5*, 1070. (d) Percec, V.; Holerca, M. N.; Uschida, S.; Cho, W.-D.; Lee, Y.; Yeardley, D. J. P. *Chem.—Eur. J.* **2002**, *8*, 1106.

(12) Percec, V.; Ahn, C.-H.; Barboiu, B. *J. Am. Chem. Soc.* **1997**, *119*, 12978.

(13) (a) Prokhorova, S. A.; Sheiko, S. S.; Ahn, C.-H.; Percec, V.; Möller, M. *Macromolecules* **1999**, *32*, 2653. (b) Percec, V.; Holerca, M. N. *Biomacromolecules* **2000**, *1*, 6. (c) Percec, V.; Holerca, M. N.; Yeardley, D. J. P.; Ungar, G. *Biomacromolecules* **2001**, *2*, 729. (d) Percec, V.; Bera, T. K. *Biomacromolecules* **2002**, *3*, 167.

(14) Bao, Z.; Amudson, K. R.; Lovinger, A. J. *Macromolecules* **1998**, *31*, 8647.

(15) Sato, T.; Jiang, D.-L.; Aida, T. *J. Am. Chem.* **1999**, *121*, 10658.

(16) (a) Kwon, Y. K.; Chvalun, S. N.; Blackwell, J.; Percec, V.; Heck, J. A. *Macromolecules* **1995**, *28*, 1552. (b) Percec, V.; Schlueter, D.; Ronda, J. C.; Johansson, G.; Ungar, G.; Zhou, J. P. *Macromolecules* **1996**, *29*, 1464. (c) Chvalun, S. N.; Blackwell, J.; Cho, J. D.; Kwon, Y. K.; Percec, V.; Heck, J. A. *Polymer* **1998**, *39*, 4515. (d) Chvalun, S. N.; Blackwell, J.; Cho, J. D.; Bykova, I. V.; Percec, V. *Acta Polym.* **1999**, *50*, 51. (e) Prokhorova, S. A.; Sheiko, S. S.; Ahn, C.-H.; Percec, V.; Möller, M. *Macromolecules* **1999**, *32*, 2653. (f) Pao, W.-J.; Stetzer, M. R.; Heiney, P. A.; Cho, W.-D.; Percec, V. *J. Phys. Chem. B* **2001**, *105*, 2170. (g) Jung, H.-T.; Kim, S. O.; Ko, Y. K.; Yoon, D. K.; Hudson, S. D.; Percec, V.; Holerca, M. N.; Cho, W.-D.; Mosier, P. E. *Macromolecules* **2002**, *35*, 3717.

(17) (a) Jakubiak, R.; Bao, Z.; Rothberg, L. *Synth. Met.* **2000**, *114*, 61. (b) Jakubiak, R.; Bao, Z.; Rothberg, L. *Synth. Met.* **2001**, *116*, 41.

(18) Tietze, L.-F.; Eicher, T. *Reaktionen und Synthesen im Organischen-Chemischen Praktikum*; Thieme: New York, 1984.

(19) Coulson, D. R. *Inorg. Synth.* **1972**, *13*, 121.

(20) Hayashi, T.; Konishi, M.; Kumada, M.; Higushi, T.; Hirotsu, K. *J. Am. Chem. Soc.* **1984**, *106*, 158.

(21) Andreopoulou, A. K.; Kallitsis, J. K. *Macromolecules* **2002**, *35*, 5808.

(22) Stein, R. S.; Rhodes, M. B. *J. Appl. Phys.* **1960**, *31*, 1873.

(23) Percec, V.; Cho, W.-D.; Ungar, G.; Yeardley, D. J. P. *Angew. Chem., Int. Ed.* **2000**, *39*, 1597.

(24) (a) Grayson, S. M.; Fréchet, J. M. J. *Chem. Rev.* **2001**, *101*, 3819. (b) Hawker, C. J.; Fréchet, J. M. J. *J. Am. Chem. Soc.* **1990**, *112*, 7638.

(25) Miyaura, N.; Suzuki, A. *Chem. Rev.* **1995**, *95*, 2457.

(26) Percec, V.; Kawasumi, M. *Macromolecules* **1993**, *26*, 3917.

(27) Förster, S.; Neubert, I.; Schlüter, D. A.; Lindner, P. *Macromolecules* **1999**, *32*, 4043.

(28) Pakula, T.; Saijo, K.; Hashimoto, T.; Kawai, H. *Macromolecules* **1985**, *18*, 1294.

(29) Zhang, A.; Okrasa, L.; Pakula, T.; Schlüter, A. D., to be published.

(30) (a) Schrauwen, C.; Pakula, T.; Wegner, G. *Macromol. Chem.* **1992**, *193*, 11. (b) Kakali, F.; Kallitsis, J.; Pakula, T.; Wegner, G. *Macromolecules* **1998**, *31*, 6190.

(31) McCarthy, T. F.; Witteler, H.; Pakula, T.; Wegner, G. *Macromolecules* **1995**, *28*, 8350.

MA035688P